1-1-1992

AN ITERATIVE INTERLACING APPROACH FOR SYNTHESIS OF COMPUTER-GENERATED HOLOGRAMS

0. K. Ersoy
Purdue University School of Electrical Engineering

J. Y. Zhuang
Purdue University School of Electrical Engineering

J. Brede
Tellabs, Inc.

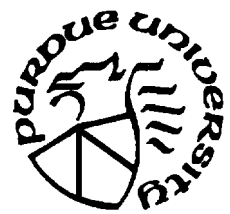

An Iterative Interlacing Approach for Synthesis of Computer-Generated Holograms

O. K. Ersoy
J. Y. Zhuang
J. Brede

TR-EE 92-2
January 1992

AN ITERATIVE INTERLACING APPROACH FOR SYNTHESIS OF COMPUTER-GENERATED HOLOGRAMS

O. K. Ersoy, J. Y. Zhuang

Purdue University

School of Electrical Engineering

W. Lafayette, IN 47907

and

J. Brede

Tellabs, Inc.

4951 Indiana Ave.

Lisle, IL 60532

Abstract

A new approach to optimizing computer-generated holograms (CGH's) is discussed. The approach can be summarized most generally as hierarchically designing a number of holograms to add up coherently to a single desired reconstruction. In the case of binary holograms, this approach results in the interlacing (IT) and the iterative interlacing (IIT) techniques. In the IT technique, a number of subholograms are designed and interlaced together to generate the total binary hologram. The first subhologram is designed to reconstruct the desired image. The succeeding subholograms are designed to correct the remaining error image. In the IIT technique, the remaining error image after the last subhologram is circulated back to the first subhologram, and the process is continued a number of sweeps until convergence. The IT and the IIT techniques can be used together with most CGH synthesis algorithms, and result in substantial reduction in reconstruction error as well as increased speed of convergence in the case of iterative algorithms.

I. Introduction

Since its invention by Brown and Lohmann in the late 1960's [1], computer-generated holograms (CGH's) have found diverse applications in many areas such as wave-shaping, optical computing and information processing, optical pattern recognition, interferometry, synthesis of novel optical elements, laser scanning, laser machining, hybrid diffractive-refractive optical elements and 3-D image display. CGH's offer advantages over conventional bulk optical elements such as compactness, light-weight, low replication cost, ability to modulate complicated wavefronts, and physical availability at any wavelength.

A major difficulty in implementing CGH's is the present status of technology for spatial amplitude and phase modulation of wavefronts. Increasingly, lithographic techniques developed for solid state semiconductor technology, such as photolithography and electron-beam lithography, is being used for the generation of CGH's [2],[3]. Spatial light modulators (SLM's) are also used for real-time processing even though they have currently low resolution and low light efficiency [4]. In all such technologies, quantization of both the amplitude and the phase of the desired wavefront is a necessity. Often, binary quantization is used, for example, (0,1) quantization indicating transmittance or no transmittance, and (-1,1) quantization indicating phase modulation as 0 or π radians. Phase quantization is usually preferable over amplitude quantization since it leads to higher diffraction efficiency. Several levels of masking with technologies such as e-beam lithography and reactive-ion etching make four- and eight-level phase quantization possible in practice at visible wavelengths [5].

Quantization is a nonlinear process. Hence, nonlinear techniques of optimization have been developed for the

Quantization is a nonlinear process. Hence, nonlinear techniques of optimization have been developed for the synthesis of CGH's. Some of these techniques are projection onto constraint sets (POCS) [6],[7],[8],[9], error diffusion [10], and direct binary search (DBS) [11].

In this article, we discuss a new approach to the nonlinear optimization of CGH synthesis, based on interlacing of subholograms to generate a total hologram. The techniques developed are quite effective in reducing reconstruction error because of the nonlinear nature of quantization. The interlacing technique (IT) generates a number of subholograms, with each subsequent subhologram being designed to reduce the reconstruction error obtained previously. The iterative interlacing technique (IIT) involves designing all the subholograms successively, and then repeating the process a number of times until the reconstruction error is not reduced further.

The experimental implementation of both the IT and the IIT techniques are first discussed in a symmetric configuration which allows both the holographic wavefront and the image wavefront to be real. In this configuration, Fourier transform reduces to the cosine transform (CT). In addition, the POCS algorithm is used. The resulting algorithm will be referred to as the POCS-CT algorithm. With this algorithm, it is especially easy to achieve the coherent addition of multiple wavefronts generated by the set of subholograms according to the IT and the IIT techniques.

The article consists of 8 sections. Section II discusses the POCS-CT algorithm. In section III, the IT technique of CGH synthesis is introduced. Section IV covers the experimental results with the IT technique. Section V introduces the IIT technique of CGH synthesis. Section VI describes experimental results with the IIT technique. Section VII is a discussion of why the IIT technique is quite effective in reducing reconstruction error. Section VIII is conclusions.

II. The POCS-CT Algorithm

In the POCS-CT algorithm, both the hologram and the image wavefronts are treated as real (or all in phase except for π phase shift) by using Hermitian symmetry.

In Fourier transform holography, the front and the back focal planes of a lens are used as the hologram and the image planes. Then, the transformation between the two planes is essentially the Fourier transform, which is approximated in numerical computations by the discrete Fourier transform (DFT). Hence, we will describe the POCS-CT algorithm below in terms of discrete-space signals and discrete-space transforms.

For the sake of simplicity, the sampled image wavefront $x(\cdot,\cdot)$ at the focal plane will be treated as real and symmetric:

$$x(n_1,n_2)=x(N_1-n_1,N_2-n_2) \tag{1}$$

where N_1 and N_2 are the number of sampling points used along the x- and y-directions. The sampling distance is assumed to be 1. **Eq.** (1) implicitly assumes that $x(n_1,n_2)$ is periodic in both directions in addition to being symmetric:

$$x(n_1,n_2)=x(N_1+n_1,N_2+n_2) \tag{2}$$

Then, **Eq.** (1) is actually the same as

$$x(n_1,n_2)=x(-n_1,-n_2) \tag{3}$$

Eq. (3) shows that the signal is symmetric with respect to the origin. With such a signal, the 2-D DFT reduces to the 2-D discrete symmetric cosine transform (DSCT) of the second kind [12]:

$$X(n_1,n_2)=\frac{4}{N_1N_2}\sum_{k_1=0}^{N_1-1}\sum_{k_2=0}^{N_2/2}x(k_1,k_2)v(k_2)\cos\left[2\pi\left(\frac{n_1k_1}{N_1}+\frac{n_2k_2}{N_2}\right)\right] \quad (4)$$

where

$$v(k_2)=\begin{cases}1/2 & k_2=0,N_2/2\\ 1 & \text{otherwise}\end{cases} \quad (5)$$

The inverse transform is:

$$x(n_1,n_2)=\sum_{k_1=0}^{N_1-1}\sum_{k_2=0}^{N_2/2}X(k_1,k_2)\cos\left[2\pi\left(\frac{n_1k_1}{N_1}+\frac{n_2k_2}{N_2}\right)\right] \quad (6)$$

It is straightforward to show that $X(n_1,n_2)$ also satisfies Eqs. (1) through (3).

The POCS algorithm is incorporated by dividing the image plane into four quadrants, as shown in Fig. 1. Two quadrants are allowed to contain the desired image and its mirror image through the origin, and the other two quadrants are allowed to be a random image and the corresponding mirror image through the origin, respectively. The rest of the procedure for the POCS-CT algorithm for the synthesis of a binary hologram is as follows:

A. $X(n_1,n_2)$ is computed according to eq. (4).

B. $X(n_1,n_2)$ is binarized according to

$$X'(n_1,n_2)=\begin{cases}1 & X(n_1,n_2)\geq 0\\ 0 & \text{otherwise}\end{cases} \quad (7)$$

C. The 2-D inverse DSCT of $X'(n_1,n_2)$ is computed according to eq. (6) to give $x'(n_1,n_2)$.

D. The reconstruction error is computed using the minimum mean-square error formula [11] rederived in the Appendix for convenience:

$$MSRE(x)=\frac{1}{N^2}\sum_{(n_1,n_2)\in I}\sum\left|x(n_1,n_2)-\lambda x'(n_1,n_2)\right|^2 \qquad (8)$$

where λ is a scaling parameter as discussed in Appendix A, and the summation is over the image quadrant (or the image region if the desired image occupies a smaller region than a quadrant). Eq. (8) is what is used in the rest of the paper to compare various results.

E. The image quadrants (quadrants 1 and 3 in Fig. 1) are set equal to the desired image. The remaining two quadrants are allowed to retain their current values. This results in an updated sequence $\tilde{x}(n_1,n_2)$:

$$\tilde{x}(n_1,n_2)=\begin{cases}x(n_1,n_2) & \text{for } n_1,n_2\in I\\ x'(n_1,n_2) & \text{otherwise}\end{cases} \qquad (9)$$

F. Steps A through E are repeated until convergence or until an error criterion is met.

The convergence of the POCS-CT algorithm can be proven in the same way as the convergence of the iterated phase methods[8]. The speed of convergence of the method has been tested in the generation of the CGH for a 128x128 edge-enhanced binary cat-brain image shown in Fig. 2. The convergence was assumed to be obtained when the absolute difference Δ_i between the successive reconstructions x_{i-1} and x_i,

$$\Delta_i=\sum_{n_1=0}^{N_1-1}\sum_{n_2=0}^{N_2-1}\left|x_i(n_1,n_2)-x_{i-1}(n_1,n_2)\right| \qquad (10)$$

is zero. The experimental results are shown in Table 1. It is observed that convergence is obtained rapidly within 9 iterations.

The POCS-CT algorithm can be compared to the POCS algorithm in which the constraint in the image domain is to restrict the image amplitude to a desired value and to allow the phase to float [7]. This method will be referred to as Hirsch method in the recainder of the paper. Such a comparison is shown in Table 2 with the same cat-brain image, in which the POCS-CT reconstruction error is observed to be larger than the POCS algorithm with random phase. This is not surprising since random phase allows an extra degree of freedom. The POCS-CT algorithm can actually be extended by allowing the phase to be random in the desired image domain while still forcing the total image to have Hermitian symmetry [13]. Then, the hologram is still real [13]. The main reason why random phase reduces reconstruction error is that the dynamic range of amplitude variations in the hologram domain are significantly reduced.

III. The Interlacing Technique

The major source of reconstruction error from CGH's is the quantization of amplitude and phase during the synthesis of the CGH. Consider the possibility of having multiple holograms designed to add up coherently to a single desired image. Each hologram can be coded coarsely, but all the holograms can be added linearly in the end so that the total number of quantization levels equals the desired number of quantization levels, whether they are for amplitude or phase.

We will consider the following strategy: the first hologram is designed to reconstruct the desired image. It results in an actual reconstructed image $x_{rec}^1(n_1,n_2)$. The error image is

$$e_1(n_1,n_2)=x(n_1,n_2)-\lambda_1 x_{rec}^1(n_1,n_2) \qquad (11)$$

The second hologram is designed to reconstruct $-e_1(n_1,n_2)/\lambda_1$. Since the optical system is linear, the sum of the two reconstructions would yield null error if the second hologram were perfect and the normalization factor is λ_1. This being not the case, the total reconstruction yields an error image $e_2(n_1,n_2)$ with a normalization factor of λ_2 for both subholograms. A third hologram is designed to reconstruct $-e_2(n_1,n_2)/\lambda_2$ yielding an error image $e_3(n_1,n_2)$. This process is continued, say, for M holograms.

In the rest of the paper, we will consider binary quantization only. Each hologram point is 0 or 1. This means it is not possible to add up M holograms for M>1 since each hologram has to be at least binary-coded. Hence, the only possibility to superpose a number of holograms is to

subholograms are designed as discussed above and interlaced together to generate the total hologram.

It is observed that initially 1/M of the total number of hologram points are utilized to reconstruct the desired image, resulting in relatively large reconstruction error. As subsequent subholograms are successively included to reduce the reconstruction error, the final result is a mean-square reconstruction error which is hopefully less than the mean-sqare reconstruction error if the total hologram was allocated as a whole without subdivisions. In the following sections, the IT technique is indeed shown to yield better performance.

A major design consideration is the interlacing geometry. A geomety with two subholograms is shown in Fig. **3.** The first subhologram consists of the odd-indexed rows, and the second subhologram consists of the even-indexed rows. This can be generalized to M subholograms. Then, each subhologram contains every Mth row of the total hologram. Obviously, the rows replaced by columns can be considered the same geometry.

A second interlacing geometry can be considered to be the checkerboard pattern shown in Fig. 4. for M=2. The experimental results with these two geometries are discussed in the next section. A large number of other geometries are possible, and it is an important research topic to determine which geometry is optimal.

IV. Experiments with the Interlacing Technique

The experiments were mostly performed with the first geometry discussed above. The desired image was the cat-brain image of Fig. 2. The number M of subholograms was chosen equal to a power of 2. Thus, M equals 2^k, k an integer.

Each subhologram has to be designed by a particular CGH synthesis technique. In the first set of experiments to be reported in this section, the POCS-CT algorithm was chosen for this purpose.

Experiments were conducted for k=0,1,···, 7. The k=O case corresponds to no interlacing. The results for the first geometry discussed in the last section are shown in Table 3. In this and all succeeding tables, the MSRE results are normalized with respect to the k=O POCS-CT MSRE. Based on the results of Table 3, the following observations can be made:

i) All of the interlacing cases (k>0) yield less MSRE than the noninterlacing case (k=0).

ii) The MSRE decreased until k≥2, and then increased again. This indicates that there is an optimal number of subholograms, and a larger subdivision of the total hologram results in suboptimal performance.

An example of the binary holograms generated with a postscript laser printer is shown in Fig. 5. The optical reconstructions for k=O and k=4 after photoreduction of the printer outputs are shown in Figs. 6 and 7. The visual observations led to the following additional conclusions:

iii) The interlacing technique causes more of the reconstruction error to be "pushed" to the non-image quadrants.

iv) As a result of reduced error, the overall contrast of the reconstructed image is improved.

Experiments were also carried out with the second geometry with two subholograms. The results did not yield much improvement over the POCS-CT method. This can be explained as follows [14]:

For a single hologram (k=0), the reconstructed image is given by Eq. (6) without any quantization. For the IT technique with the second geometry, the first subhologram is used for reconstructing the desired image and has

$$X'(n_1,n_2)=\begin{cases} X(n_1,n_2) & \text{Both } (n_1,n_2) \text{ are even or odd} \\ 0 & \text{otherwise} \end{cases} \qquad (12)$$

or equivalently

$$X'(n_1,n_2)=\frac{1}{2}[(-1)^{n_1+n_2}+1]X(n_1,n_2) \qquad (13)$$

then the reconstructed image without any quantization will be

$$x'(n_1,n_2)=\frac{1}{2}[x(n_1,n_2)+x(n_1+\frac{N_1}{2},n_2+\frac{N_2}{2})] \qquad (14)$$

Thus, the reconstructed image is the sum of the desired image and the same image shifted one-half period in both x- and y-directions. This significantly 'distorts the reconstruction since the two images overlap each other.

For the second subhologram, which is used to reconstruct the error image, the situation is the same. The distortions reduce the effectiveness of error reduction by

interlacing. This example shows the importance of sampling geometry.

It is interesting to observe that the same problem also exists in the first geometry. However, the shift of the image corresponding to the second term in Eq. (14) is in the x-direction or the y-direction only. This means the shifted image is in the region where the random image exists, and the random image also moves to the region of the desired image and may cause problems. This is why it was important initially to zero the random image regions.

V. The Iterative Interlacing Technique

Let $e_f(n_1,n_2)$ be the final error image with the IT technique together with the final normalization factor λ_f. In the iterative interlacing technique (IIT), this error is circulated back to the first subhologram to reduce the MSRE further (actually the ordering in which the subholograms are reactivated can be chosen in many ways). This is done by letting the desired image for the first subhologram to generate be

$$x_1'(n_1,n_2)=x_{rec}^1(n_1,n_2) - e_f(n_1,n_2)/\lambda_f \quad (15)$$

The new error image is

$$e_1'(n_1,n_2)=x_1'(n_1,n_2)-\lambda_1' x_{rec}^{1'}(n_1,n_2) \quad (16)$$

The second subhologram is designed to reconstruct $x_{rec}^2(n_1,n_2)-e_1'(n_1,n_2)/\lambda_1'$, where λ_1' is the normalization factor after the first subhologram during the second sweep. It yields a new error image $e_2'(n_1,n_2)$. A third subhologram is designed to reconstruct $x_{rec}^3(n_1,n_2)-e_2'(n_1,n_2)/\lambda_2'$, where λ_2' is the normalization factor after the second subhologram during the second sweep. This process is continued for all the subholograms. One such run through all the subholograms is called a sweep. A number of sweeps is carried out until convergence or until some error criterion is met.

VI. Experiments with the Iterative Interlacing Technique

The experimental results with the IIT technique for the cat-brain image when the subholograms were designed by the POCS-CT algorithm are shown in Table 4. These results lead to the following conclusions:

i) In all cases considered, the IIT results give considerable further gains over the IT results alone.

ii) The MSRE decreased significantly in the first 3 or 4 sweeps and then leveled off.

iii) The minimum MSRE occurred at a larger number of subholograms (k=5) as compared to the IT technique. For larger k, the MSRE remains stable.

iv) In Table 4, 8 sweeps are shown since more number of sweeps led to very little reduction in the MSRE. There were no further reductions after 15 sweeps.

Both the IT and the IIT techniques can be used with other CGH synthesis algorithms for the subholograms. We experimented with Hirsch's method and the DBS algorithm together with the IIT method.

The results with Hirsch's method are shown in Table 5. As expected, the MSRE is considerably lower than with the POCS-CT algorithm. Otherwise, the overall trends are very similar to the results in Table 4, but the gains obtained with the IIT technique are even more pronounced: 45% further reduction in the MSRE is obtained after 5 sweeps.

The results with the DBS algorithm are shown in Table 6, in comparison to the results with the POCS-CT algorithm. A major concern with the DBS algorithm is the computation time, which grows very fast with the hologram size. Because of this, the size of the cat-brain image was reduced to 64X64 by undersampling. It is observed that the IIT method reduces the MSRE by a small margin over the DBS method alone after 3-4 sweeps. More interestingly, the computation time is reduced to about 1/5 of the DBS method alone. We also observe that k=1 case has the smallest MSRE while k=2 case has the smallest computation time. It can be concluded that the DBS algorithm can be considerably improved, especially in terms of computation time by proper choice of the number of subholograms.

VII. Discussion

We believe that the main reason for the superior performance of the IIT technique together with a particular CGH synthesis algorithm over the performance of the CGH synthesis algorithm by itself is the ability of the IIT technique to reach a deeper minimum of the MSRE function, and possibly also at a faster pace.

The IIT technique resembles simulated annealing to reach the global minimum of a nonlinear energy or error function [15]. In simulated annealing, the temperature parameter T is initially kept high, allowing wrong moves on a stochastic basis. This serves the purpose of avoiding getting trapped in a local minimum. As iterations increase, T is reduced, and more and more correct moves reducing the value of the energy function is allowed. Similarly, in the IIT technique, initially one subhologram is active for optimization, leading to a suboptimal minimization of the MSRE. As more and more subholograms are activated, more optimal minimization of the MSRE is obtained, but the procedure is still suboptimal at each time point since only one subhologram is active. As the sweeps increase, minimization of the MSRE becomes more optimal since each subhologram is contributing closer to its best performance. The IIT technique appears to reach a deep minimum because of gradual increase in optimality as described above. Whether this minimum is the global minimum or close to the global minimum requires further research to determine. It is known that deep minima obtained by the DBS algorithm are very close to the global minimum [11]. Since the IIT results are comparable to the DBS results, the minima obtained by the IIT technique are indeed expected to be close to the global minimum.

In terms of performance and granularity of the hologram, the IIT results together with the synthesis techniques discussed in the previous sections resemble the DBS results. The IIT algorithm also resembles the error diffusion algorithm since hologram apertures are successively and iteratively designed by attempting to reduce error. However, the error considered is in the image domain rather than the hologram domain, and error reduction is carried out by a whole subhologram rather than being cell-oriented.

The IIT algorithm also resembles the cyclic coordinate descent (CCD) algorithm in optimization theory [16]. However, CCD involves freezing all variables except one at each step of optimization, and is known to be very slow. In contrast, IIT uses a subhologram with many variables to be optimized, and is experimentally observed to converge considerably faster than the case when all the variables are simultaneously being optimized. This has been observed to be especially striking in the case of the DBS algorithm.

The discussion above implies that the approach of dividing resources in subgroups and allocating each subgroup in the same way as the subholograms are allocated should work well in a number of nonlinear optimization problems. We observed this to be the case in transform image coding [17] and neural networks [18].

VIII. Conclusions

The IT and the IIT technique together with a particular CGH synthesis algorithm appears to be very effective in reducing the MSRE over what is achievable with the CGH synthesis algorithm alone, in addition to speeding up the convergence time.

The MSRE was reduced by the IIT technique together with Hirsch's method by about 45% over Hirsch's method alone, and by about 27% with the POCS-CT method over the POCS-CT method alone. When the IIT technique was used together with the DBS algorithm, the improvement in the MSRE was small since the DBS algorithm is very efficient, but the reduction in computation time was about 5 times. This feature is expected to be especially useful with large hologram sizes.

The IIT technique is believed to be a general strategy valid in nonlinear optimization problems. Its ability to reach deep minimum and its fast convergence speed makes it a potential approach for solving a number of large-scale problems involving nonlinear optimization.

Appendix

The mean square error (MSE) is defined between the original image x and the reconstructed image x' as

$$MSRE(x)=\frac{1}{N^2}\sum_{(n_1,n_2)\in I}\sum\left|x(n_1,n_2)-\lambda x'(n_1,n_2)\right|^2 \qquad (A.1)$$

where λ is a constant scaling factor. λ for which the MSRE is minimized is found by taking the partial derivative of Eq. (A.l) with respect to λ and setting this derivative equal to zero:

$$\lambda=\frac{\sum_{(n_1,n_2)\in I}\sum x(n_1,n_2)(x'(n_1,n_2))^*}{\sum_{(n_1,n_2)\in I}\sum |x'(n_1,n_2)|^2} \qquad (A.2)$$

Acknowledgement

This research was partially supported by G. R. Dodge Foundation under grant no. 670 1285-1258, Allied Signal and Purdue Optoelectronics Center under grant no. 670 1285-2187.

References

1. B. R. Brown, A. W. Lohmann, "Complex Spatial Filtering with Binary Masks", Applied Optics, Vol. 5, No. 6, pp. 967-969, June 1966.

2. O. K. Ersoy, " Construction of Point Images with the Scanning Electron Microscope: A Simple Algorithm", Optik, Vol. 46, pp. 61-66, September 1976.

3. W. B. Veldkamp, G. J. Swanson, "Developments in Fabrication of Binary Optical Elements", Proc. SPIE on Int. Conf. Computer-Generated Holography, Vol. 437, pp. 54-59, August 1983.

4. J. Amako, T. Sonehara, " Kinoform Using an Electrically Contronlled Birefringent Liquid-Crystal Spatial Light Modulator", Applied Optics, Vol. 30, No. 32, pp. 4622-4628, 10 November 1991.

5. S. J. Walker, J. Jahns, "Array Generation with Multilevel Phase Gratings," J. Optical Society of America A, Vol. 7, No. 8, pp. 1509-1513, August 1990.

6. H. Stark, ed., Image recovery: Theory and Applications, Academic Press, 1986.

7. P. M. Hirsch, L. B. Lesem, J. A. Jordan, "Method of Making an Object-Dependent Diffuser", U. S. Patent No. 3,619,022, 1971.

8. B. Liu, N. C. Gallagher, "Convergence of a Spectrum Shaping Algorithm", Applied Optics, Vol. 13, No. 11, pp. 2470-2471, November 1974.

9. N. C. Gallagher, B. Liu, "Method for Computing Kinoforms that Reduces Image Reconstuction Error", Applied Optics, Vol. 12, No. 10, pp. 2328-2335, October 1973.

10. S. Weissbach, F. Wyrowski, O. Bryngdahl, "Digital Phase Holograms: Coding and Quantization with an Error Diffusion Concept", Opt. Commun., Vol. 72, pp. 37-41, 1989.

11. M. A. Seldowitz, J. P. Allebach, D. W. Sweeney, "Synthesis of Digital Holograms by Direct Binary Search", Applied Optics, Vol. 26, No. 14, pp. 2788-2798, 15 July 1987.

12. O. K. Ersoy, Y. Yoon, N. Keshavo, D. Zimmerman, "Nonlinear Matched Filtering II", Optical Engineering, Vol. 29, No. 9, pp. 1002-1012, September 1990.

13. S. Naqvi, private communication.

14. J. Allebach, private communication.

15. S. Kirkpatrick, C. D. Gelatt, M. P. Vecchi, "Optimization by Simulated Annealing", Science, Vol. 220, No. 4598, pp. 671-680, May 1983.

16. D. G. Luenberger, Introduction to Linear and Nonlinear Programming, Addison-Wesley, 1973, and 1984.

17. S. Aghagolzadeh, O. K. Ersoy, "Optimal Multistage Transform Image Coding", IEEE Tran. Circuits and Systems for Video Technology, December 1991.

18. O. K. Ersoy, S-W Deng, "Parallel, Self-Organizing, Hierarchical Neural Networks with Continuous Inputs and Outputs", Report No. TR-EE-91-51, Purdue University, and submitted to IEEE Tran. Neural Networks.

Table 1. Convergence of the POCS-CT algorithm.

Iteration	Δ
1	1893716
2	808075
3	436190
4	236840
5	112340
6	84050
7	45130
8	20535
9	0

Table 2. Comparison of the POCS algorithms.

	POCS Algorithms	
	POCS (Hirsch)	POCS-CT
MSRE	0.556	1.000

Table 3. Mean-Square Reconstruction Error with the Interlacing Technique.

	k=O	k=1	k=2	k=3	k=4	k=5	k=6	k=7
MSRE	1.000	0.909	0.907	0.909	0.918	0.927	0.929	0.936

Table 4. Mean-Square Reconstruction Error with the IIT Technique as a Function of the Number of Sweeps and the Number of Subholograms When the Subholograms Are Designed by the POCS-CT Algorithm (Image Size is 256x256).

Error / k / Sweeps	MSRE							
	k=O	k=I	k=2	k=3	k=4	k=5	k=6	k=7
1	1.000	0.909	0.907	0.909	0.918	0.927	0.929	0.936
2		0.845	0.802	0.780	0.805	0.807	0.809	0.809
3		0.812	0.770	0.745	0.768	0.767	0.768	0.768
4		0.793	0.758	0.752	0.753	0.751	0.751	0.751
5		0.784	0.756	0.745	0.746	0.743	0.744	0.744
6		0.783	0.748	0.742	0.742	0.739	0.740	0.739
7		0.777	0.747	0.740	0.739	0.736	0.737	0.737
8		0.773	0.745	0.739	0.738	0.735	0.735	0.736

Table 5. Mean-Square Reconstruction Error with the IIT Technique as a Function of the Number of Sweeps and the Number of Subholograms When the Subholograms Are Designed by Hirsch's Method (Image Size is 256x256).

Error / k / Sweeps	MSRE							
	k=0	k=l	k=2	k=3	k=4	k=5	k=6	k=7
1	0.556	0.494	0.495	0.496	0.508	0.521	0.528	0.537
2		0.405	0.375	0.369	0.369	0.375	0.376	0.382
3		0.367	0.343	0.334	0.331	0.332	0.331	0.335
4		0.349	0.332	0.321	0.318	0.316	0.31 5	0.319
5		0.341	0.328	0.315	0.313	0.310	0.309	0.31 1
6		0.336	0.324	0.313	0.310	0.307	0.306	0.307
7		0.333	0.323	0.311	0.308	0.305	0.304	0.305
8		0.332	0.321	0.310	0.307	0.304	0.302	0.304

Table 6. Mean-Square Reconstruction Error and Computation Time with the IIT Technique as a Function of the Number of Sweeps, the number of Subholograms, and the Computation Time When the Subholograms Are Designed by the DBS algorithm or the POCS-CT algorithm (Image Size is 64x64).

Sweeps \ k	Error	MSRE and Computation Time (Sec.)							
		k=0		k=1		k=2		k=3	
		POCS-CT	DBS	POCS-CT	DBS	POCS-CT	DBS	POCS-CT	DBS
1	MSRE	1.000	0.644	0.859	0.732	0.877	0.805	0.899	0.840
	CPU(s)	0.06	27.34	0.13	1.71	0.06	1.89	0.15	5.14
2	MSRE			0.786	0.674	0.760	0.683	0.756	0.714
	CPU(s)			0.13	3.27	0.10	2.69	0.17	6.03
3	MSRE			0.742	0.642	0.725	0.651	0.709	0.665
	CPU(s)			0.14	4.55	0.11	3.25	0.19	6.64
4	MSRE			0.736	0.634	0.705	0.639	0.696	0.644
	CPU(s)			0.15	5.44	0.11	4.33	0.20	7.22
5	MSRE			0.731	0.623	0.700	0.635	0.687	0.637
	CPU(s)			0.15	6.40	0.11	5.22	0.20	7.76
6	MSRE			0.730	0.619	0.695	0.630	0.683	0.633
	CPU(s)			0.19	8.63	0.12	5.96	0.23	8.26
7	MSRE			0.726	0.618	0.690	0.627	0.676	0.632
	CPU(s)			0.19	10.04	0.14	6.75	0.24	11.32
8	MSRE			0.726	0.615	0.687	0.625	0.674	0.631
	CPU(s)			0.20	12.29	0.15	9.07	0.27	12.05

Note: CPU time valid up to 0.1s

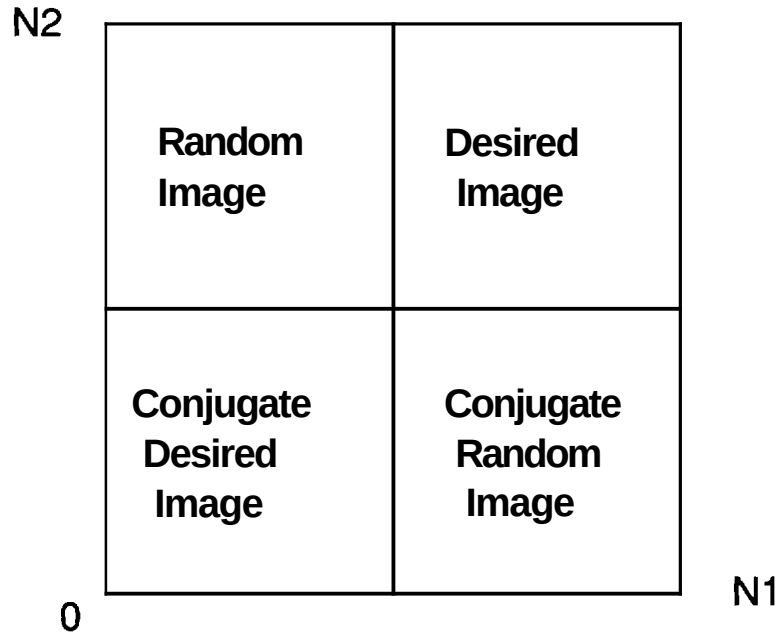

Fig.l. Hermitian Symmetry Used in the POCS-CT Algorithm.

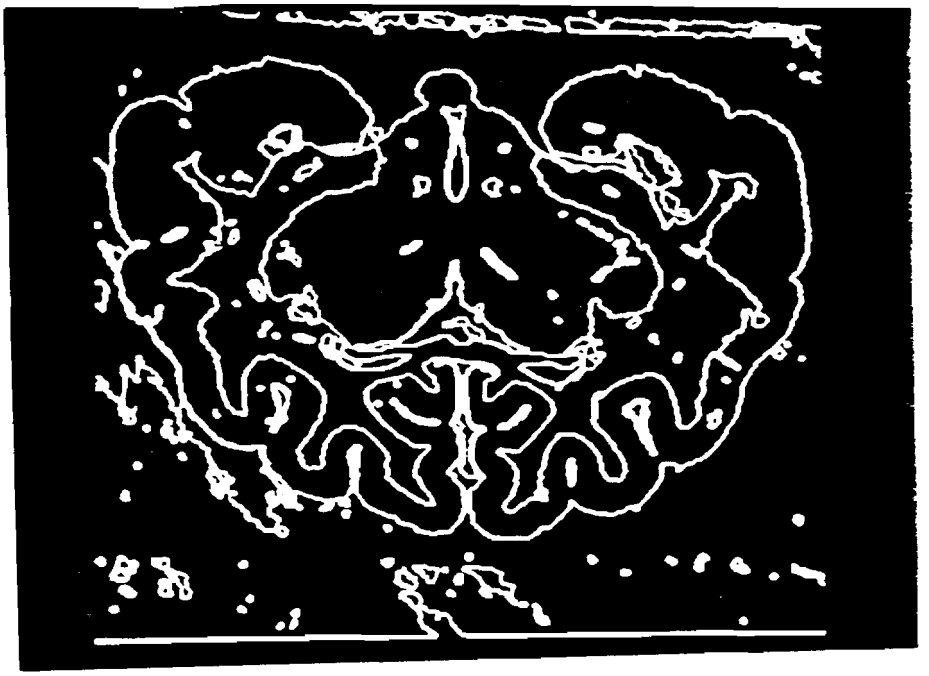

Fig. 2. The Edge-Enhanced Cat Brain Cross-Section Image of Size 128x128.

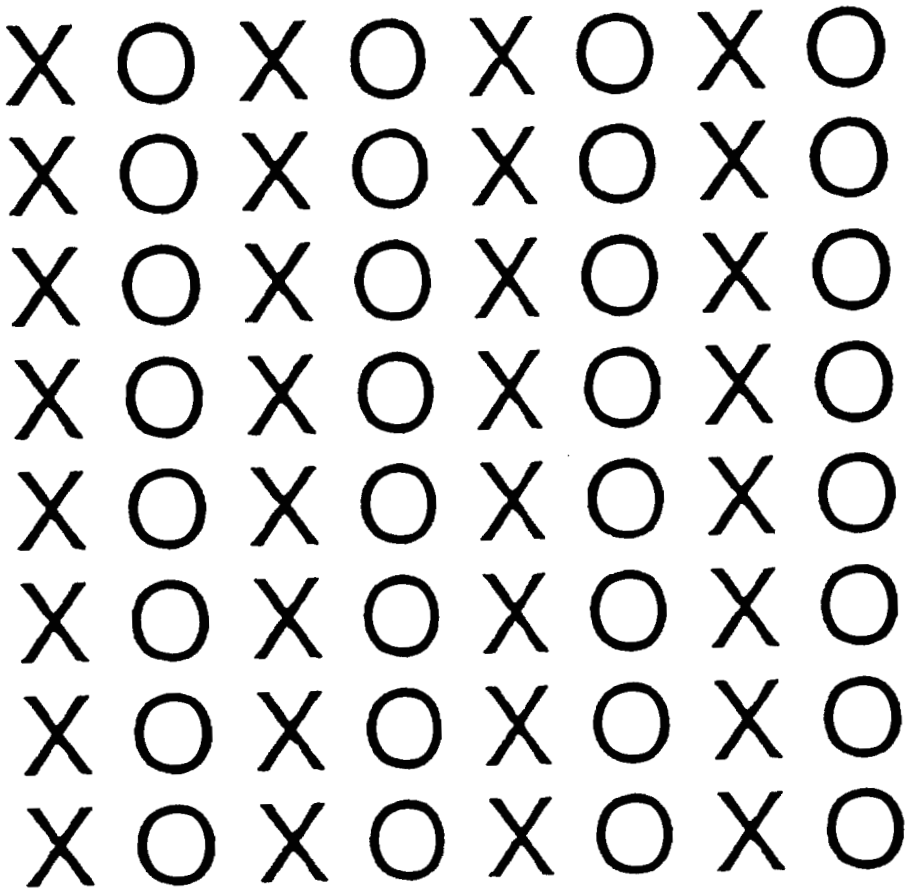

Fig. **3.** The Interlacing Geometry Used in the IT and the IIT Techniques.

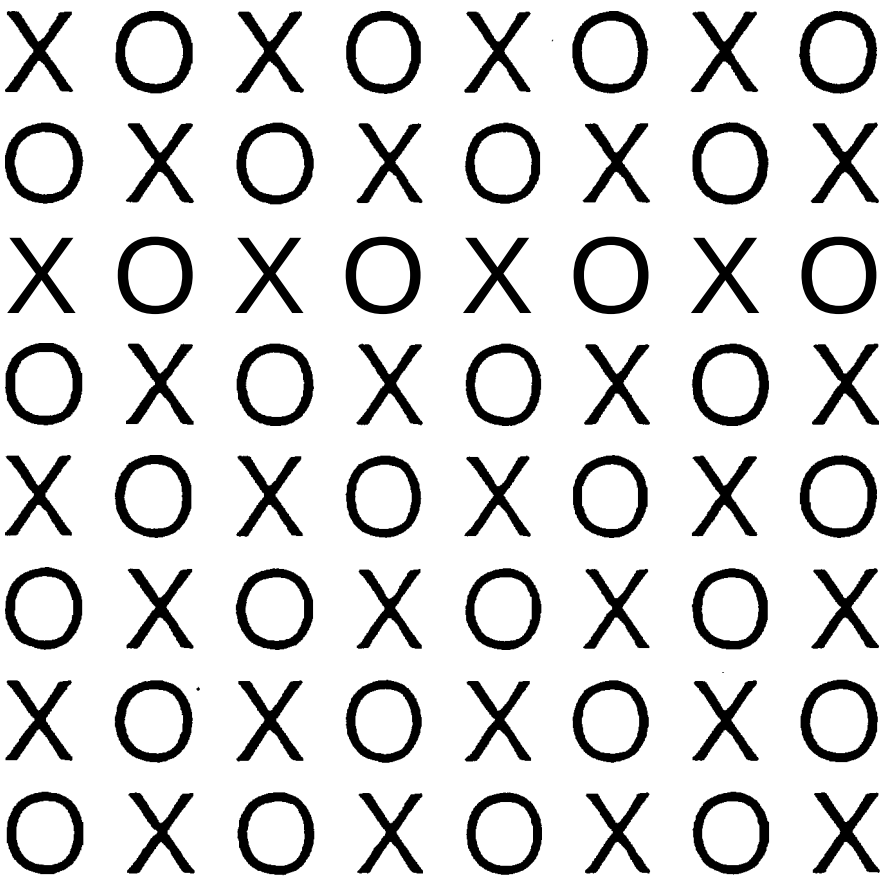

Fig. 4. Another Interlacing Geometry Used in the IT and the IIT Techniques.

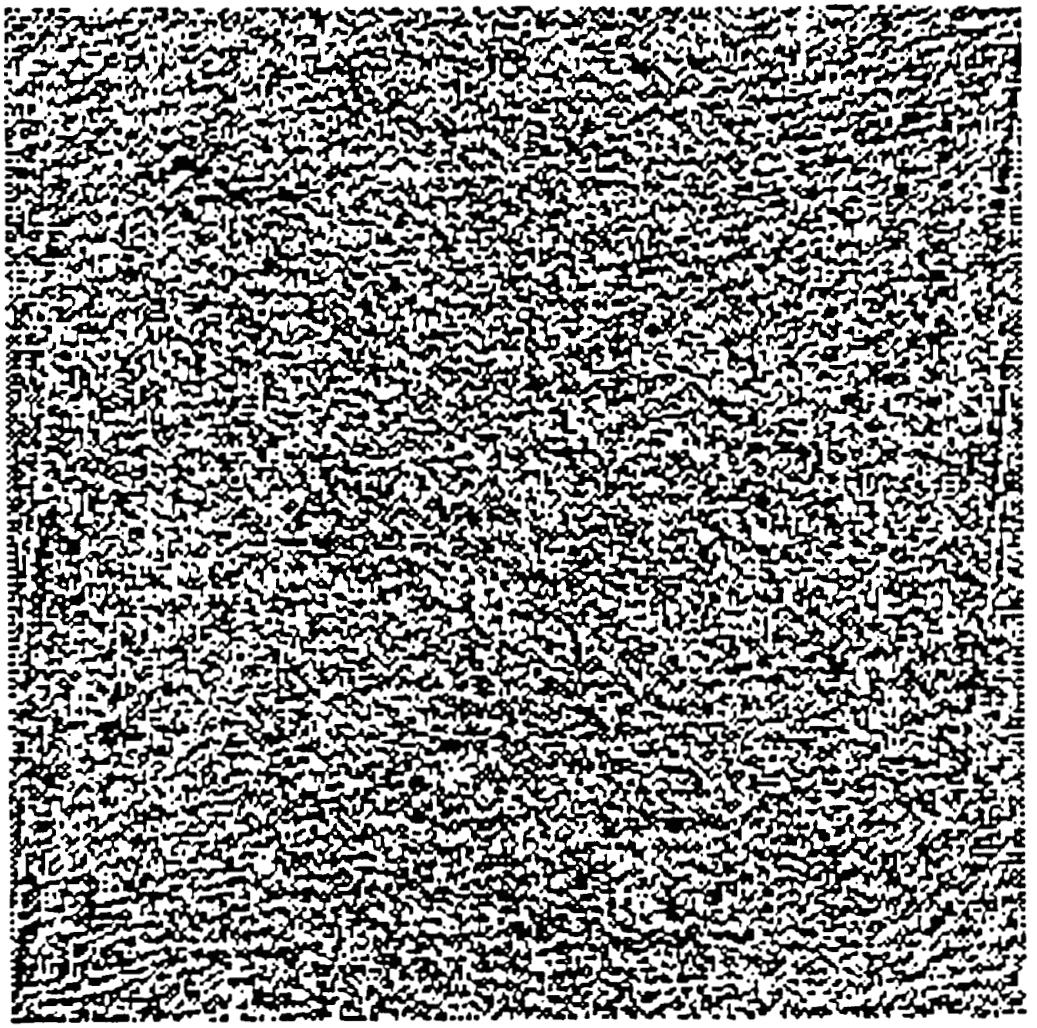

Fig. 5. **A** Binary Hologram Generated by the Interlacing Technique.

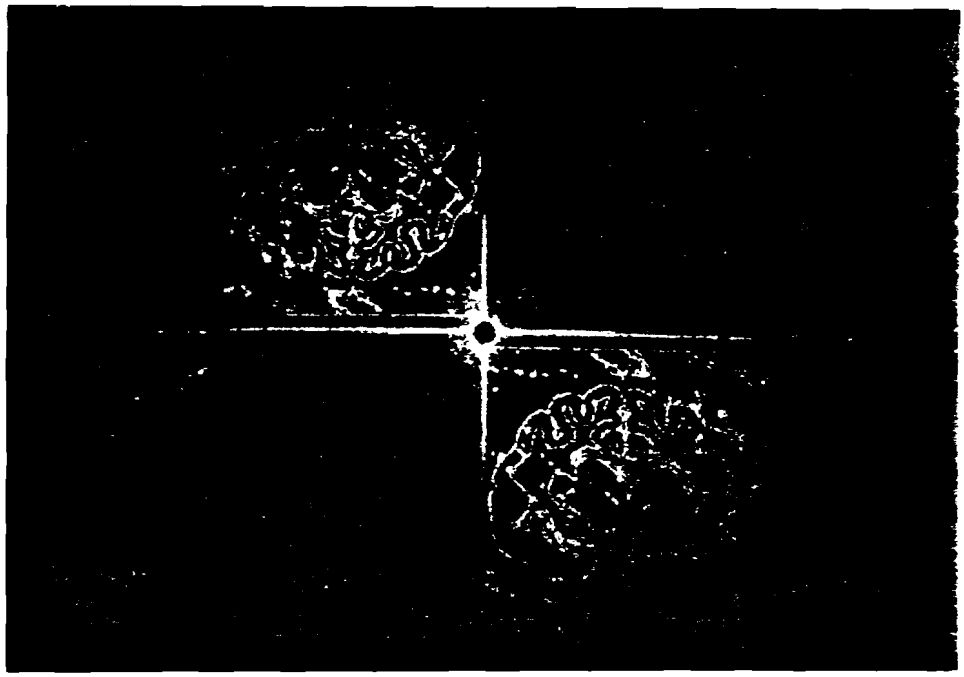

Fig. 6. The Optical Reconstruction of the Cat Brain Image When the Hologram is Designed by the POCS-CT Algorithm.

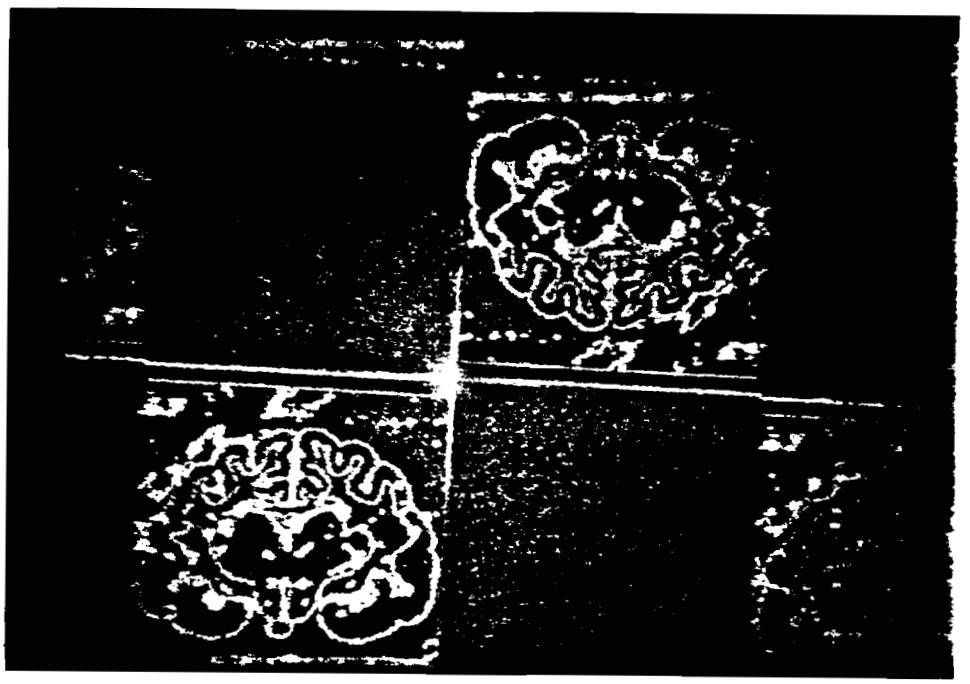

Fig. 7. The Optical Reconstruction of the Cat Brain Image When the Hologram is Designed by the IT Technique together with the POCS-CT Algorithm and the Number of Subholograms is 8.